

3. H. Kondo. Response of a Circular Cylindrical Tank to Earthquakes. Presented at Symposium on Lifeline Earthquake Engineering, Portland, Ore., June 1983.
4. K.M. Nova and A. Hindy. Dynamic Response of Buried Pipelines. Proc., 6th European Conference on Earthquake Engineering, Dubrovnik, Yugoslavia, Sept. 1978.
5. J.Q. Burns and R.M. Richards. Attenuation of Stresses for Buried Cylinders. Proc., Symposium on Soil-Structure Interaction, University of Arizona, Tucson, Sept. 1964.
6. R.E. Elling, S.Y. Tuann, and W.S. Tseng. Stresses in Cylinders Embedded in a Stressed Soil Field. Proc., Fourth Canadian Conference on Earthquake Engineering, Vancouver, June 1983.
7. K. Hoeg. Stresses Against Underground Structural Cylinders. Journal of the Soil Mechanics and Foundation Division, ASCE, July 1968.
8. G.N. Savin. Stress Concentration Around Holes (translated by E. Gros). Pergamon Press, London, 1961.
9. S.K. Chan and I.S. Tuba. A Finite Element Method for Contact Problems of Solid Bodies. International Journal of Mechanical Sciences, Vol. 13, 1971.
10. R.E. Goodman, R.C. Taylor, and T. Brekke. A Model for the Mechanics of Jointed Rock. Proc., ASCE, Vol. 92, No. SM3, May 1966.
11. S.K. Arya and G. Hegemier. Finite Element Method for Interface Problems. Proc., ASCE, Vol. 108, No. ST2, Feb. 1982.
12. M.G. Katona. A Simple Contact-Friction Interface Element with Application to Buried Culverts. International Journal of Numerical and Analytical Methods in Geomechanics, Vol. 7, No. 3, 1983.
13. R.E. Elling. Stresses in Buried Cylindrical Tanks. Department of Civil Engineering Report 8S-83. Clemson University, Clemson, S.C., Dec. 1983.
14. S.P. Timoshenko and J.N. Goodier. Theory of Elasticity, 3rd ed. McGraw-Hill Book Company, New York, 1970.

Publication of this paper sponsored by Committee on Subsurface Soil-Structure Interaction.

## Tensile Properties of Chemically Grouted Sand

CUMARASWAMY VIPULANANDAN and RAYMOND J. KRIZEK

### ABSTRACT

Although the tensile properties (strength, stiffness, failure strain, and mode of failure) of grouted soils are important in many soil-structure interaction problems, little effort has been directed toward identifying and quantifying the mechanisms responsible for the manifested behavior. In this study chemically grouted sand is considered as a two-phase particulate composite, and the tensile properties are examined at both the particulate and the composite levels. Both the adhesive and cohesive properties of the grout are seen to influence the behavior of grouted sand, and an experimental program was conducted to quantify particular relationships for each. These data, together with the porosity of the sand, are employed to formulate two strength models for predicting the tensile behavior of a grouted sand from a knowledge of the properties of the constituents. Comparisons are made between the tensile and compressive properties of grout and grouted sand, and the development of cracks within the specimen is offered as an explanation for the observed nonlinearity in the stress-strain response when either grouted sand or pure grout cured for more than about 2 weeks is tested in compression.

The increasing use of chemical grouting to solve problems involving soil-structure interaction (tunnel support, underpinning, anchors, etc.) has dictated that more efficient design procedures be developed and that a better understanding of grouted sand behavior under different loading conditions be achieved. Although much current design is based on

the assumption that the material can resist only compression and shear forces, tensile forces are encountered in many cases. Interest in the tensile properties of stabilized materials has also been stimulated by efforts to provide crack-free liners for waste ponds and cut-offs for dams. In general, many geomaterials have little tensile strength, and

grouted sand is known to behave in a similar manner. However, the extent to which the cohesive or adhesive properties of the grout, or both, influence the tensile behavior of the grouted sand composite is not well known and needs to be quantified.

#### OBJECTIVES

The objectives of this study are (a) to quantify experimentally the variations in the tensile properties of grout and grouted sand with curing time, (b) to evaluate the contributions of the sand, grout, and interface bond to the overall behavior of the grouted sand, (c) to develop strength relationships for both the grout and the grouted sand under tensile loading conditions, and (d) to use the properties of the constituents in the formulation of a model for predicting the tensile response of grouted sand.

#### MATERIALS

Inasmuch as the main purpose of this study was to develop an improved understanding of the underlying mechanisms responsible for the tensile behavior of grout and grouted sand, the materials were limited to one grout and one sand. The grout consisted of hydrated sodium silicate ( $\text{Na}_2\text{SiO}_3 \cdot n\text{H}_2\text{O}$ ), water ( $\text{H}_2\text{O}$ ), formamide ( $\text{HCONH}_2$ ), and ethyl acetate ( $\text{CH}_3\text{COOC}_2\text{H}_5$ ) proportioned according to volume in the ratio of 8:10:1:1. The sand was Ottawa 20-30, which is composed almost entirely of pure quartz.

#### TESTING TECHNIQUES

Because there are currently no standard tests to evaluate the tensile properties of either the grout or the sand-grout composite, testing techniques used for other materials were modified and adapted to obtain the required measurements. Two types of test were employed--one to measure the tensile properties and the other to measure the adhesive or bond strength.

##### Tension Tests

In general, testing techniques used to study material behavior in tension can be categorized as either direct or indirect tests. The direct tensile test is the oldest and possibly the only test that satisfies the condition of uniaxial tension on which the definition of tensile stress is based. In its simplest form this test consists of molding a specimen in a simple geometric shape (such as a cylinder, prism, or briquette) with or without enlarged ends and applying a tensile force in the direction of the longitudinal axis until the material fails. In a direct tensile test, gripping of the specimen is a crucial problem and the success of the test depends in large part on the effectiveness of this gripping. Problems normally encountered in a direct tensile test are misalignment, stress concentrations, and eccentricities in loading. If the study is to include stress-strain behavior, there are additional constraints in selecting the shape of the test specimen, because stresses and strains must be as uniform as possible. The main advantage of a direct tensile test is that material properties need not be assumed in determining the average stresses and strains within the specimen.

Several indirect tensile test methods have been developed to study the tensile strength of brittle materials; of these, hollow cylinder tests and split tensile tests [used by Skipp and Renner (1, pp.29-33) for grouted sand] are the most common. Although some of the methods for indirect testing appear simple, there is widespread disagreement among investigators regarding the reproducibility of results (2). Although some of the shortcomings of direct tensile tests can be overcome by indirect tensile tests, the latter also have their limitations. Perhaps the most significant is that the stress-strain response of a material cannot be studied unless some material properties are assumed.

In this experimental program the direct tensile test with cylindrical specimens and the particular configuration shown in Figure 1(a) was used. Other specimen shapes (such as the briquette and the tapered cylinder) were rejected because of the difficulty in making them and the problems in maintaining uniform stresses or strains or both.

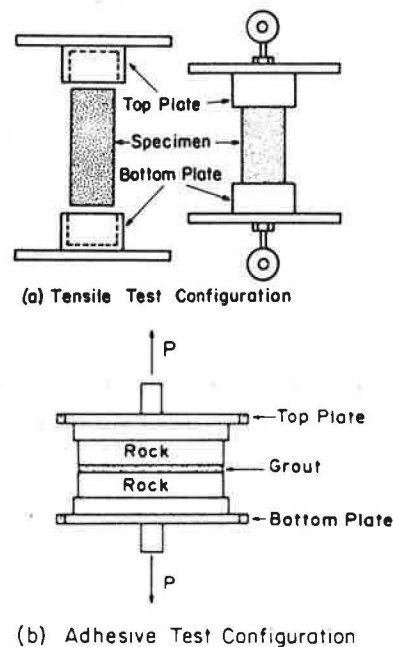


FIGURE 1 Test configurations.

##### Adhesion Tests

When two or more materials interact at their interface because of physical or chemical reasons or both, the resulting condition is known as adhesion or bonding. In the case of sand and grout, not only is the type of bonding unknown for many grouts, but the long-term stability of the interface bonding is not well understood. To determine the strength at the interface under tension, tests must be conducted under conditions in which the interfacial stresses are uniform over the major, if not the entire, portion of the interface. In addition, it is highly desirable that the interfacial stress state be simple, so that a simple and correspondingly useful strength value is obtained. However, problems are encountered when an attempt is made to meet such conditions, because a complex state of stress invariably arises at the interface whenever a system consisting of two mechanically distinct, but integral, phases is loaded externally.

Tensile tests are commonly used for evaluating adhesives, and ASTM has several standards for determining the adhesive tensile strength. The specimen configuration described by ASTM D897 suggests that the adhesive tensile strength can be obtained from a so-called pi tensile test, in which adhesive is placed between two flat circular plates with a cross-sectional area of 6.5 cm<sup>2</sup>. For this test configuration, the stress distribution of the interface will be uniform only if the moduli of the adherend and the adhesive are equal. Any difference in these moduli results in the transmittal of a shear stress across the interface (3).

Because the bonding properties of grout and quartz sand are of concern here, the sand surface was modeled by a quartz rock surface, in which the chemical composition of the rock was similar to that of the sand. The test consisted of sandwiching a layer of grout between flat surfaces of quartz rocks, as shown in Figure 1(b), and subjecting the entire system to a tensile load at the appropriate curing time. Flat rock surfaces were obtained by sawing 50.8-mm-diameter rock cores and gluing them with epoxy to aluminum plates.

TENSILE PROPERTIES OF GROUT

Three series of six pure grout (PG) specimens were

tested in direct tension after different periods of curing in a humid temperature-controlled room. These specimens were prepared in a 15.2-cm-long, 38.4-mm-diameter polyvinylchloride tubes, which were closed with rubber stoppers at the bottom and sealed at the top with wax paper. In preparation for testing, each specimen was trimmed, centered, and glued to the end plates with epoxy. The specimens were loaded at a strain rate of 0.15 percent per minute in a modified GEONOR testing machine, and both load and displacement were measured. The tensile stress ( $\sigma_t$ ) was calculated as  $P/A$ , where  $P$  is the tensile load and  $A$  is the cross-sectional area of the specimen. The study was limited to curing periods of 1 month, and typical test results are shown in Figure 2.

The stress-strain relationship for PG specimens under tensile loading was found to be linear for all curing times investigated. All specimens failed in tension (that is, the failure plane was perpendicular to the axis of loading and away from the end plates), and values for the strength, failure strain, and modulus for all three series of tests are summarized in Figure 3. The tensile strength increased continuously with curing time at a reducing rate; the 7-day strength (1.8 kg/cm<sup>2</sup>) increased by 50 percent after 14 days and an additional 25 percent after 28 days of curing. Although the failure strain increased with curing time, the rate of in-

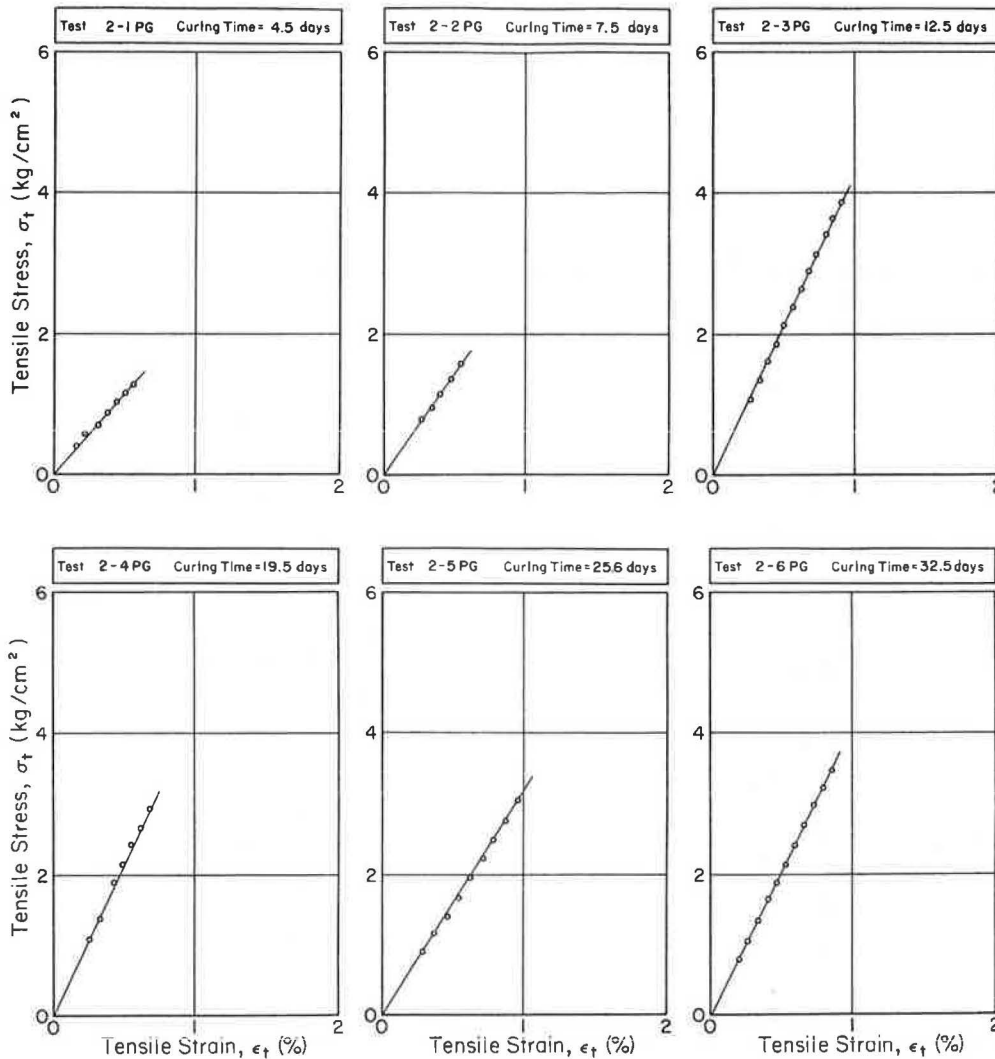


FIGURE 2 Tensile stress-strain relationships for pure grout at different curing times.

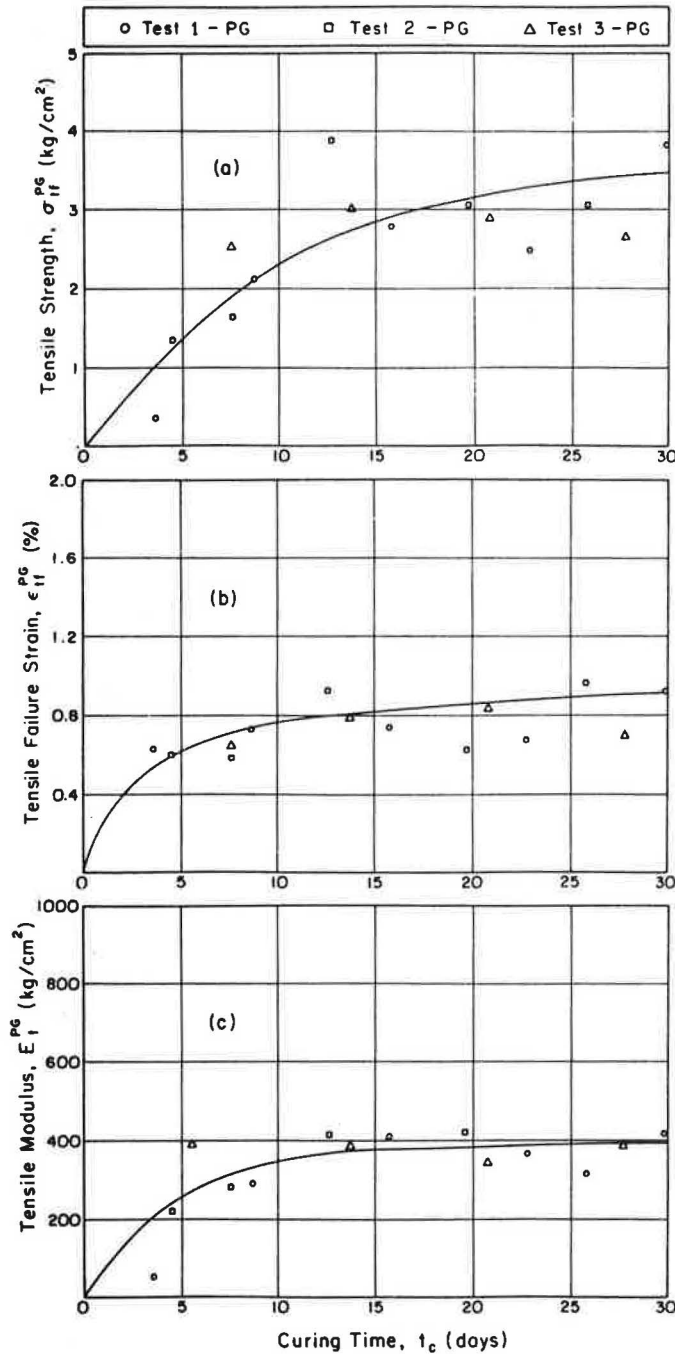


FIGURE 3 Variation of tensile strength, failure strain, and modulus with curing time.

crease slowed greatly after 2 weeks of curing. Similar trends were observed for the tensile modulus; the 7-day modulus of 300 kg/cm<sup>2</sup> increased by 20 percent after 14 days and a further 10 percent after 28 days of curing.

INTERFACE BOND

For the type of test shown in Figure 1(b), equilibrium considerations dictate that the average adhesive tensile (AT) stress at failure ( $\sigma_{ff}^{AT}$ ) across the interface in the axial direction must be  $P/A$ ,

where  $P$  is the maximum applied load and  $A$  is the cross-sectional area. Of course, the maximum stress may be larger because of stress concentrations. Figure 4 summarizes the adhesive tensile strength as a function of curing time for five series of tests. The strength increases rapidly during the first week or so and reaches a peak value of about 5 kg/cm<sup>2</sup>. However, with increased curing the strength reduces by about 20 percent after 3 to 4 weeks. This reduction may be due to (a) a continuous chemical reaction at the interface or (b) a partial debonding and development of high residual stresses as the grout shrinks and becomes brittle or (c) both of the foregoing reasons.

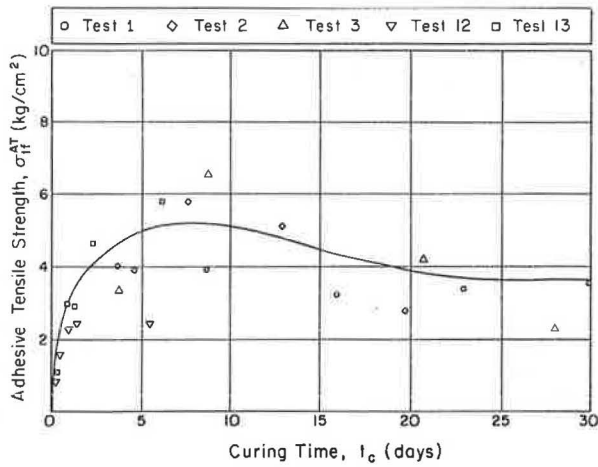


FIGURE 4 Variation of adhesive tensile strength with curing time.

TENSILE PROPERTIES OF GROUTED SAND

Because of the lack of a standard method for specimen preparation, grouted sand specimens for laboratory studies have been prepared in many different ways in the past. However, Christopher (4) has shown that the method of preparation has an influence on the properties of a grouted sand. In general, laboratory specimens should be prepared in a way that closely resembles field conditions; accordingly, injecting grout into a sand confined under  $K_0$  conditions is recommended and was used here. A known amount of sand was placed in a longitudinally split Plexiglas tube (38 mm in diameter and 90 mm long) and then vibrated to obtain a porosity of  $0.36 \pm 0.02$ . Six specimens were grouted in parallel at an injection pressure of approximately 13.8 kPa; several void volumes of grout were passed through each specimen. Approximately 1 day after grouting, the molds were dismantled and the specimens were removed, sealed in moistened plastic bags, and stored in a humid room at a temperature of  $20^\circ\text{C} \pm 2^\circ\text{C}$ .

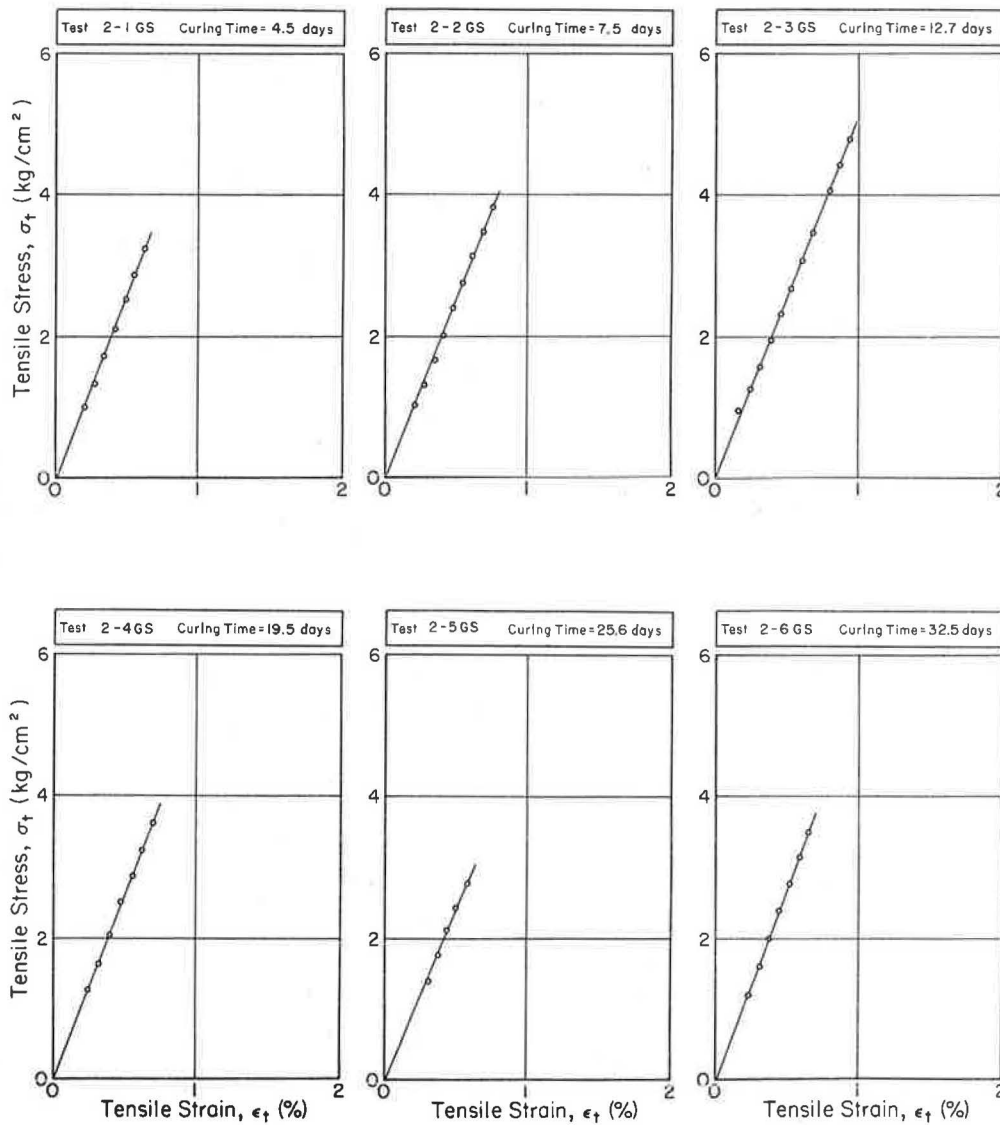


FIGURE 5 Tensile stress-strain relationships for grouted sand.

The test program on these specimens of grouted sand was similar to that used for pure grout; after appropriate periods of curing, three series of six specimens were loaded at a strain rate of 0.15 percent per minute. The stress-strain relationship for grouted sand under monotonic tensile loading is typically linear, as shown in Figure 5. All specimens failed in tension, and inspection of the failure plane (by using a magnifying glass with a magnification factor of 3) showed both adhesive and cohesive failures. The variation of tensile properties obtained from these tests is shown in Figure 6. The strength increased continuously at a reducing rate for about 2 weeks, after which it slowed slightly and appeared to approach a constant value of about 3.5 kg/cm<sup>2</sup>. The failure strain also increased continuously at a reducing rate for about 2

weeks to a value of about 0.8 percent and then remained almost constant for another 2 weeks. Although the initial rate of increase in the modulus was not measured, it attained a value of about 500 kg/cm<sup>2</sup> after 4 days and remained essentially constant thereafter.

COMPARISONS

Because most of the available mechanical property data on grouts and grouted sands have been obtained from compression tests, it is useful to advance some comparisons (albeit tentative and based on limited data) between tensile and compressive properties. Toward this end, solid cylindrical specimens (38 mm in diameter and 85 mm in height) of pure grout and grouted sand were capped with a sulfur compound and tested in unconfined compression at a strain rate of 0.15 percent per minute; the comparisons in the form of compressive/tensile ratios are given in Table 1.

TABLE 1 Ratios of Compressive to Tensile Properties

Curing Time (days)	Pure Grout			Grouted Sand		
	Strength	Failure Strain	Modulus	Strength	Failure Strain	Modulus
7	1.4	—	0.5	4.1	1.0	7.3
14	2.8	2.3	1.5	4.2	0.5	9.4
28	3.1	1.2	2.8	4.1	0.4	10.0

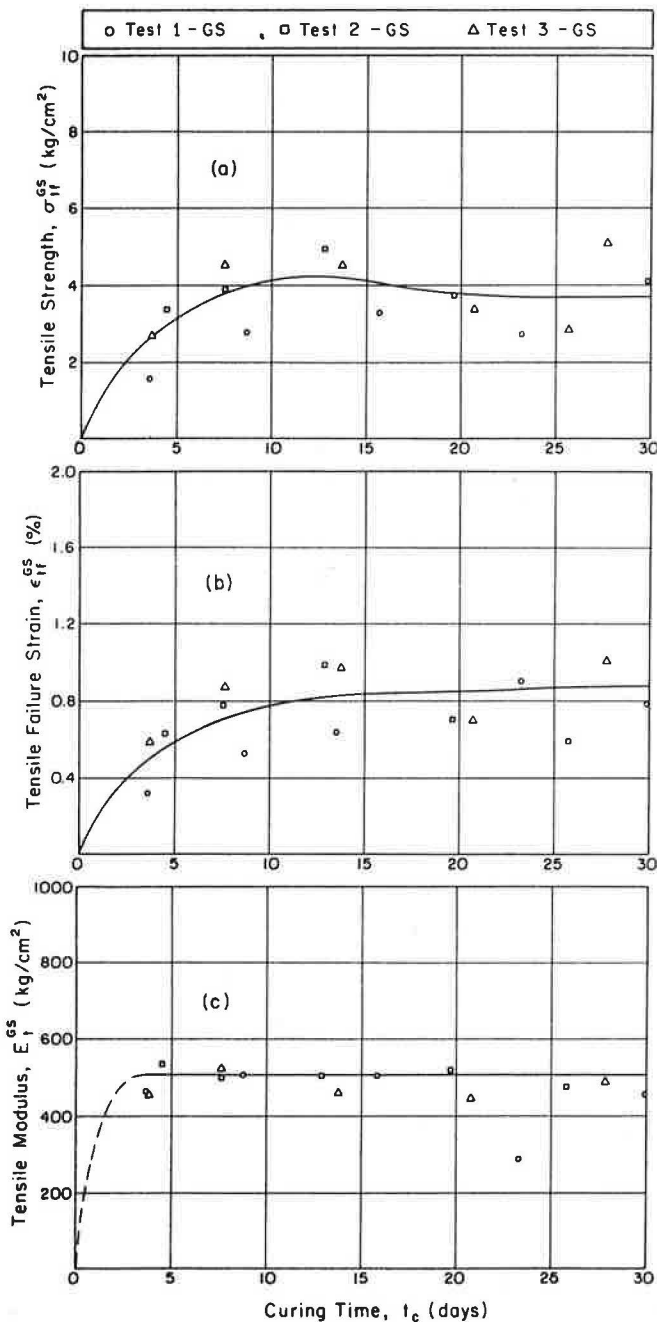


FIGURE 6 Variation of tensile properties with curing time.

Grout

For specimens of pure grout the compressive/tensile ratios increase with curing time, reaching a value of 2 after 10 to 12 days and a value of 3 after about 4 weeks. The ratio of failure strain, on the other hand, decreases and approaches unity after a month or so. The tensile and compressive moduli (measured as the slope at 50 percent strength) differ by a factor of 2 or more; the compressive modulus is less than the tensile modulus for the first 10 to 12 days of curing, whereas the opposite is true for longer curing periods. Accordingly, grout is in general a bimodulus material and there will be a discontinuity in the slope of a hysteresis curve as the stress passes from tension to compression or vice versa.

Grouted Sand

In the case of grouted sand the compressive strength during the first month of curing was consistently about four times the tensile strength, and the compressive modulus was about an order of magnitude higher (perhaps increasing somewhat with curing time). As for the specimens of pure grout, the compressive/tensile ratios of failure strain decreased with curing time, but for grouted sand the failure strain in compression was generally less than that in tension.

CRACKING IN COMPRESSION

Specimens of pure grout cured for only a few days and then subjected to unconfined compression tests were observed to behave in a nonlinear manner throughout the tests, and they failed by bulging at a large failure strain with no visible cracks on the surface. On the other hand, specimens cured for

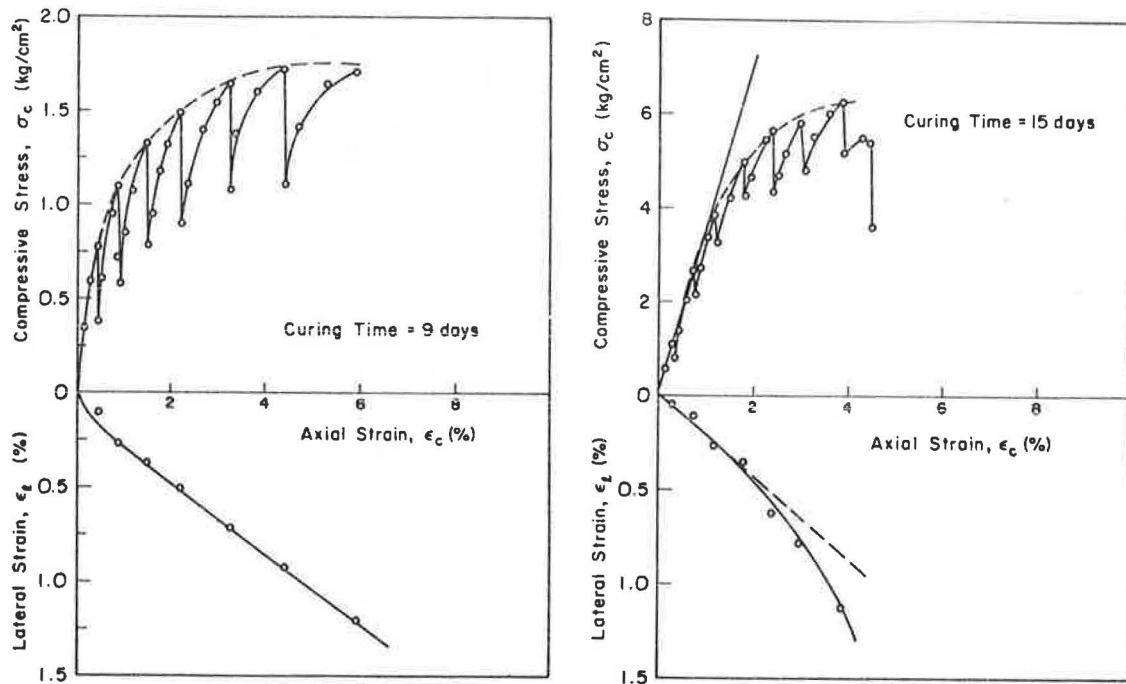


FIGURE 7 Lateral deformation of pure grout under compressive loading.

longer periods manifested an initially linear stress-strain response, which became nonlinear with increased deformation and the development of surface cracks with approaching failure at strains of less than 2 percent (5). In an effort to study (at least implicitly) the possible formation of microcracking (either internal or external), the lateral deformations were measured at the midpoint of the specimen as it was loaded. Three micrometers (each with an accuracy of 0.0025 mm, spaced 120 degrees apart, and mounted on a Lucite pressure chamber at the same level) were used to measure deformations in the lateral direction (6). As the specimens were tested, loading was stopped periodically at preselected axial strains and lateral deformations were measured. Figure 7 shows the test results for two specimens cured 9 days and 15 days. The younger specimen exhibited a more-or-less linear relationship between lateral and axial strain (with a value slightly less than 0.2 for the Poisson's ratio); this linearity suggests the absence of cracking within the specimen during loading. The older specimen manifested an initially linear relationship between lateral and axial strain (with a value slightly greater than 0.2 for the Poisson's ratio), but it became nonlinear as the axial strain increased; this suggests that cracks are forming within the specimen as loading is increased. Although the observed nonlinearity could be due to various causes, the suggestion of internal cracking is one plausible explanation. A common phenomenon in both tests is the relaxation exhibited by the grout, which indicates that it possesses a time-dependent or viscous nature.

Grouted sand manifests a distinctly nonlinear stress-strain response as the peak strength is approached. Some appreciation for the reasons underlying this behavior was obtained by studying the lateral deformations during compressive loading. Figure 8 shows the results for two specimens cured 6 days and 15 days. In both cases the lateral deformation increased rapidly in the nonlinear portion of the stress-strain curve near failure, which suggests that cracks may be forming within the specimen. Grouted sand, similar to pure grout, possesses vis-

cus properties and manifests stress relaxation under a sustained constant strain.

#### STRENGTH MODELS

To understand the macroscopic behavior of a composite material, it is sometimes desirable to study its behavior in terms of a unit element, which is the smallest representative sample of the entire mass. Because Ottawa 20-30 sand was used in this study, the sand grains can be considered as equidiameter spheres. As shown in Figure 9, a regular array of such spheres can be represented in their densest possible packing as a face-centered-cubic or tetrahedral array (porosity = 0.260), whereas a simple cubic array will give the loosest, but yet stable, packing (porosity = 0.476). This range of porosity spans that of many natural sand deposits, which have porosities between about 0.30 and 0.45. Smith et al. (7) concluded that an assembly of randomly packed spherical particles may be regarded as an arrangement of separate clusters of face-centered-cubic (FC) and simple cubic (SC) arrays, each present in a proportion to yield the observed porosity ( $n$ ) of the assembly. Thus, if  $p$  is the volumetric fraction of FC clusters, we have

$$n = pn_{FC} + (1 - p)n_{SC} \quad (1)$$

Because the porosity (measured before grouting) of the sand in this study was  $0.36 \pm 0.02$ , the volume fractions of FC and SC clusters are 0.54 and 0.46, respectively. Although it was not generally true, the grout was assumed to fill the voids as a first approximation.

Failure is defined here as the ultimate load-carrying capacity of a grouted sand specimen. At the macroscopic level, grouted sand failed in tension, but both adhesive and cohesive failures were observed on the failure surface at the microscopic level. Hull (8) reported a similar failure pattern on closely packed fiber-reinforced composites, where all cracks followed the fiber-matrix interface in

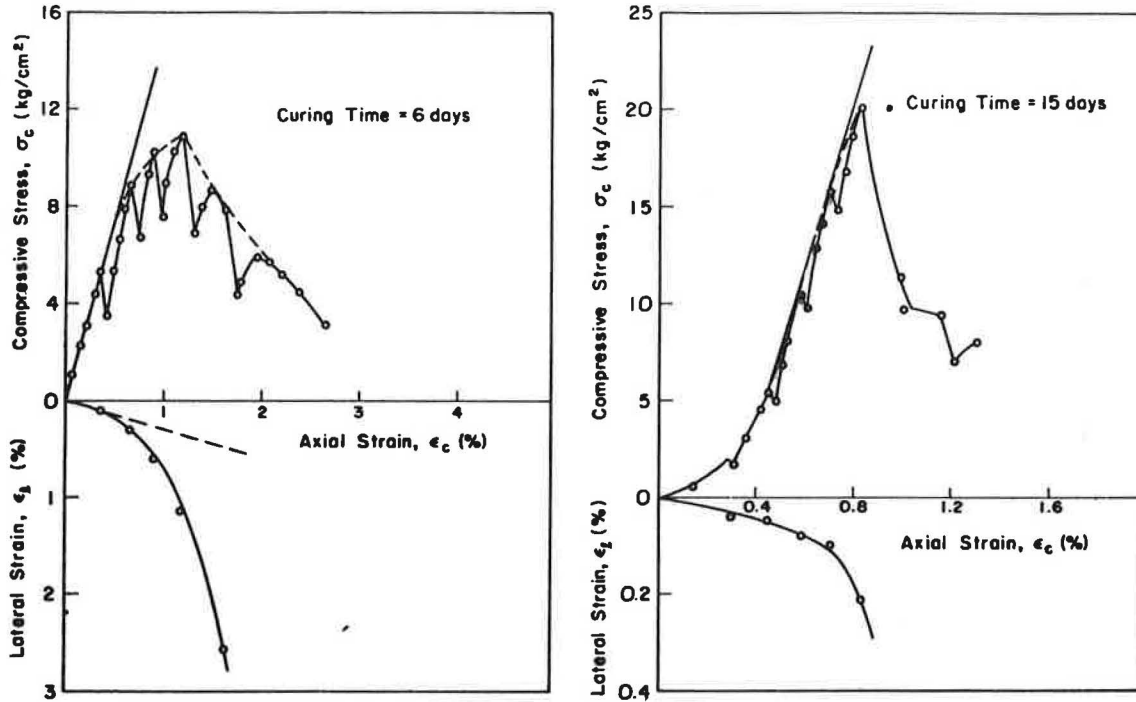


FIGURE 8 Lateral deformation of grouted sand under compressive loading.

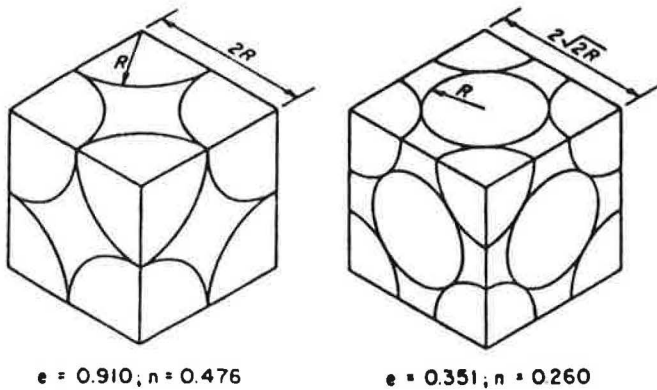


FIGURE 9 Unit elements for regular packing of sphere: simple cubic array (left) and face-centered-cubic array (right).

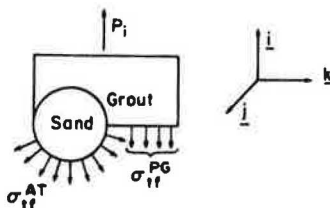


FIGURE 10 Condition of tensile failure.

the region of dense packing. At or close to tensile failure, the intergranular force on the failure surface will be zero. Hence, the effect of particle interaction on such a failure can be neglected. Because experimental observations show both adhesive and cohesive failures, the ultimate tensile load ( $P_i$ ) can be represented as

$$P_i = f_{A_S} \underline{s} \cdot \underline{\sigma}^A \cdot \underline{i} dA_S + f_{A_G} \underline{s} \cdot \underline{\sigma}^C \cdot \underline{i} dA_G \quad (2)$$

where

- $\underline{i}$  = unit vector in direction of loading,
- $A_S$  = area of sand-grout interface,
- $A_G$  = grout area on failure plane,
- $\underline{s}$  = surface normal, and
- $\underline{\sigma}^A, \underline{\sigma}^C$  = stress tensors at interface (A = adhesion) and within the grout (C = cohesion), respectively.

Within this criterion one condition for failure could be when the radial stress on the interface reaches the adhesive tensile (AT) strength of the grout ( $\sigma_{if}^{AT}$ ) and the stress in the grout reaches the tensile strength of the grout ( $\sigma_{if}^{PG}$ ) on the failure surface as shown in Figure 10. For a semisphere loaded hydrostatically, it can be shown that

$$f_{A_S} \underline{s} \cdot \underline{\sigma}^A \cdot \underline{i} dA_S = \sigma_{if}^{AT} A_{S1} \quad (3)$$

where  $A_{S1}$  is the projected sand area perpendicular to the direction of loading. Since  $\underline{\sigma}^C$  is a constant, the second part of Equation 2 can be simplified to

$$f_{A_G} \underline{s} \cdot \underline{\sigma}^C \cdot \underline{i} dA_G = \sigma_{if}^C A_{G1} \quad (4)$$

where  $A_{G1}$  is the projected grout area perpendicular to the direction of loading. Therefore, the use of Equations 3 and 4 allows Equation 2 to be written as

$$\sigma_{if}^{GS} = \sigma_{if}^{AT} (A_{S1}/A) + \sigma_{if}^{PG} (A_{G1}/A) \quad (5)$$

where  $\lambda_{if}^{GS}$  is the tensile strength of grouted sand.

When  $\sigma_{if}^{AT} \geq \sigma_{if}^{PG}$  (as in this case), we have

$$(\sigma_{if}^{GS})_{max} = \sigma_{if}^{AT} (A_{S1}/A)_{max} + \sigma_{if}^{PG} [1 - (A_{S1}/A)_{max}] \quad (6)$$



For both an FC and an SC array of sand grains,  $(A_{S1}/A)_{\max} = \pi/4$ , which enables Equation 6 to be expressed as

$$(\sigma_{tf}^{GS})_{\max}/(\sigma_{tf}^{PG}) = (\pi/4)(\sigma_{tf}^{AT}/\sigma_{tf}^{PG}) + [(4-\pi)/4] \quad (7)$$

Equation 7 will be termed Model 1. By using approximations where the stresses are considered as a form of volume average, it is possible to rewrite Equations 3 and 4 as

$$1/A \int_{A_S} s \cdot \underline{\sigma}^A \cdot \underline{i} dA_S = (V_S/V) \sigma_{tf}^{AT} = (1-n) \sigma_{tf}^{AT} \quad (8)$$

and

$$1/A \int_{A_G} s \cdot \underline{\sigma}^{PG} \cdot \underline{i} dA_G = (V_G/V) \sigma_{tf}^{PG} = n \sigma_{tf}^{PG} \quad (9)$$

With the use of Equations 8 and 9, Equation 2 can be simplified to

$$(\sigma_{tf}^{GS}/\sigma_{tf}^{PG}) = (1-n)(\sigma_{tf}^{AT}/\sigma_{tf}^{PG}) + n \quad (10)$$

Equation 10 will be called Model 2. For an FC array of sand particles, Equation 10 becomes

$$(\sigma_{tf}^{GS}/\sigma_{tf}^{PG})_{FC} = (1-n_{FC})(\sigma_{tf}^{AT}/\sigma_{tf}^{PG}) + n_{FC} \quad (11)$$

and for an SC array it may be written as

$$(\sigma_{tf}^{GS}/\sigma_{tf}^{PG})_{SC} = (1-n_{SC})(\sigma_{tf}^{AT}/\sigma_{tf}^{PG}) + n_{SC} \quad (12)$$

Combining Equations 11 and 12 with Equation 1 yields

$$\sigma_{tf}^{GS}/\sigma_{tf}^{PG} = p(\sigma_{tf}^{GS}/\sigma_{tf}^{PG})_{FC} + (1-p)(\sigma_{tf}^{GS}/\sigma_{tf}^{PG})_{SC} \quad (13)$$

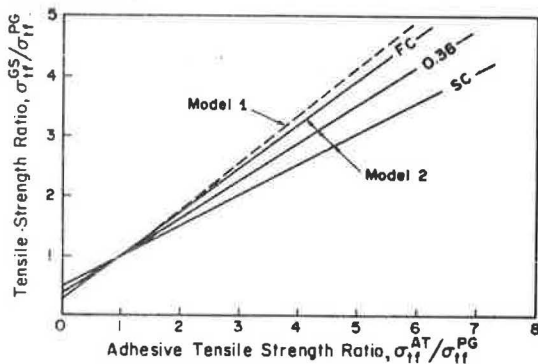


FIGURE 11 Representation of tensile strength models.

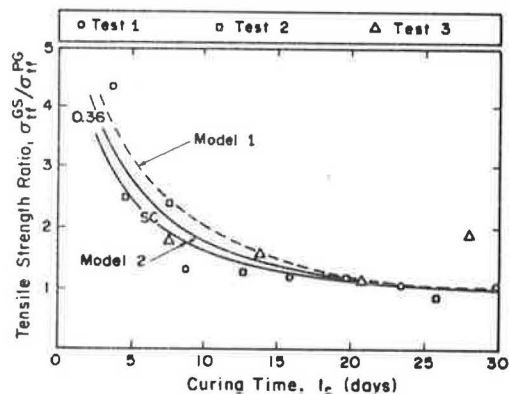


FIGURE 12 Comparison of predicted and measured tensile strength of grouted sand.

According to Equation 13, the tensile strength of a grouted sand for a particular packing of sand grains can be represented in terms of the volumetric fractions of the strengths of the two idealized arrays. In Figure 11 the results calculated from Equations 7, 10, 11, and 12 are compared, and Figure 12 shows how well the predictions of these models agree with the experimental data. Hence, these models can be used in conjunction with the adhesive and cohesive properties of grout to predict the tensile strength of grouted sand.

CONCLUSIONS

Based on this complementary experimental and analytical study, the following conclusions can be advanced:

1. The tensile strength, failure strain, and modulus of pure grout and grouted sand change continuously at varying rates during the first month of curing; the tensile strength and modulus were higher for grouted sand than for pure grout, but the failure strains were generally comparable (less than 1 percent).
2. Under monotonic uniaxial tensile loading, both grout and grouted sand manifest a linear stress-strain response and a tensile failure at the macroscopic scale; however, both adhesive and cohesive failures were observed on the failure plane of the grouted sand.
3. Adhesive tensile strength develops rapidly during the first few days of curing but decreases somewhat with increased curing; this may be due to (a) a continuous chemical reaction at the interface, (b) shrinkage of the grout and the development of high residual stresses, or (c) both.
4. Limited test data on grouted sand and pure grout cured for more than 2 weeks suggest that the nonlinear behavior in compression near peak strength is due to the formation of cracks within the specimen; because the tensile failure of grouted sand is of a brittle nature, appropriate precautions must be taken when this material is used in construction applications.
5. The unconfined compressive strength of grouted sand is about four times the uniaxial tensile strength and the modulus in compression is about 10 times that in tension; this difference is attributed in large measure to the greater particle-to-particle interactions under compressive loading.
6. Two different strength models offer the potential for predicting the tensile strength of a grouted sand from a knowledge of the adhesive and cohesive tensile properties of the grout and the porosity of the sand.

Because this study was limited to a single uniform sand and one particular grout, generalizing the observed results and the development models must be approached with caution. The usefulness of this work will be increased greatly if it is demonstrated to be applicable to other combinations of grouts and sands.

ACKNOWLEDGMENT

This study was supported in part by the National Science Foundation.

## REFERENCES

1. B. Skipp and L. Renner. The Improvement of the Mechanical Properties of Sand. Proc., Symposium on Grouts and Drilling Muds in Engineering Practice, British National Society, International Society of Soil Mechanics and Foundation Engineering, Institute of Civil Engineers, London, 1963.
2. M.M. Al-Hussaini and F.C. Townsend. Tensile Testing of Soils: A Literature Review. Miscellaneous Paper S-73-24. U.S. Army Corps of Engineers Waterways Experiment Station, Vicksburg, Miss., 1963.
3. G.P. Anderson, S.J. Bennett, and K.L. DeVries. Analysis and Testing of Adhesive Bonds. Academic Press, New York, 1977.
4. R. Christopher. Evaluation of Specimen Preparation and Testing Procedures for Chemically Stabilized Granular Materials. M.S. thesis. Department of Civil Engineering, Northwestern University, Evanston, Ill., 1979.
5. C. Vipulanandan. Interactive Roles of Constituents on the Mechanical Behavior of Chemically Grouted Sand. Ph.D. dissertation. Department of Civil Engineering, Northwestern University, Evanston, Ill., 1984.
6. R.P. Khera and R.J. Krizek. Measurement and Control of Radial Deformation in the Triaxial Test of Soils. Materials Research and Standards, Vol. 7, No. 9, 1967, pp. 392-396.
7. W.D. Smith, P.D. Foote, and P.F. Busang. Packing of Homogeneous Spheres. Physical Review, Vol. 24, 1929, pp. 1271-1274.

---

Publication of this paper sponsored by Committee on Subsurface Soil-Structure Interaction.

# California Department of Transportation Structural Steel Plate Pipe Culvert Research: Design Summary and Implementation

A. E. BACHER and D. E. KIRKLAND

## ABSTRACT

Three structural steel plate pipes (SSPP) have been instrumented and tested as part of an extensive culvert research program by the California Department of Transportation. Two were functional roadway cross drains, at Chadd Creek and Apple Canyon, and one was a grossly underdesigned culvert, the DB culvert. The Chadd Creek culvert was a 114-in. SSPP 0.280 in. thick with 89 ft of overfill and Method B backfill (baled straw surmounting the pipe). The diagram of Method B fill height versus soil stress was nonlinear; strains and strain gradients were large; deflection was 1 percent. The Apple Canyon culvert was a twin 108-in. SSPP 0.375 in. thick with 160 ft of overfill and Method A backfill (structure backfill surrounding the culvert periphery). The diagram of Method A fill height versus soil stress was linear; relatively uniform peripheral pressures were observed; there was an effective density increase of 50 percent subsequent to fill completion and 2 percent deflection. The DB culvert was a 120-in. SSPP 0.109 in. thick with a maximum of 190 ft of overfill and six zones of Method A backfill and two zones of Method B backfill. The six Method A zones suffered excessive deflections or seam failure before fill completion. The two Method B zones (with slotted bolt holes or sprayed polystyrene backpacking) reduced effective densities significantly. Conclusions for Method A are that the design loading should be 140V:140H and that the effective density increase should be 1.5. The Marston and Spangler design methods are not recommended; ring-compression and neutral-point analysis are acceptable designs. The Method B conclusions are that baled straw is not recommended and that slotted bolt holes and sprayed polystyrene show promise.